

The Treasure Chamber of the OH Megamaser Mrk 273

H. R. Klöckner^{1,2} and W. A. Baan²

¹ Kapteyn Institute, University of Groningen, P.O. Box 800, 9700 AV Groningen, The Netherlands

² ASTRON, Westerbork Observatory, P.O. Box 2, 7990 AA Dwingeloo, The Netherlands

Abstract. Line and continuum observations carried out by the EVN at 1.6 GHz show an emission structure in the central region of 1 square arcsec in the Megamaser galaxy Mrk 273. The detected hydroxyl emission reveals an unexpected view on the molecular environment, with emission up to a spatial extent of 240 mas towards only one nuclear source. The hydroxyl emission itself is partially superposed on the continuum emission and shows a moderately high main-line ratio, which suggests optically thin maser emission with a more complex pumping scheme. The line-of-sight velocities indicate the organized structure of an edge-on disk/TORUS with Keplerian rotation around a central object with a mass of $3.5 \times 10^8 M_{\odot}$. The observed continuum emission displays three individual regions with self-absorbed synchrotron radio spectra. Combined with existing HI observations they may reveal a third nucleus toward the southeast taking part in a merging scenario.

1. Introduction

Extragalactic hydroxyl (OH main-lines) emission has been studied since the early eighties (see Baan et al., 1982) revealing a new class of extragalactic masers with unexpected isotropic luminosities of several magnitudes higher than galactic OH emissions. The OH Megamaser (OH-MM) galaxies are morphologically peculiar, showing high molecular and dust contents in combination with Starburst Nuclear (SBN) and Active-Galactic-Nuclear (AGN) phenomena. Furthermore, the Megamaser galaxies are a subsample of the ultra-luminous infrared galaxies (ULIRG), which reflects the relation between the infrared and the OH emission via an hydroxyl pumping scheme (Baan, 1989). The exceptional line width of the OH emission in these galaxies are thought to trace the circumnuclear environment close to a central engine. So far only a small fraction of the OH Megamaser galaxies has been observed with very-long-baseline-interferometry (see Table 1) revealing the nuclear region and showing a more complex picture for the continuum and the maser emission. These observations detect typically up to 50 percent of the peak line flux density observed at lower resolution. Furthermore, the maser emission itself shows both compact and more extended emission components with various amplification factors and main-line ratios, which may represent saturated and unsaturated maser components.

New EVN observations of the OH line and the continuum emission in the Megamaser galaxy Mrk 273 are presented. The detailed imaging of the nuclear region shows significant substructure contributing to the general understanding of the central environment. Wherever possible a comparison with line and continuum observations at various bands have been made to reveal the kinematic and the physical properties of the nuclear region. The

Table 1. OH Megamaser galaxies recently observed at mas resolution.

Source	d[Mpc] ^a	Instrument
Arp220	73.1	VLBI ^b
IIIZw35	111.2	VLBI ^c , VLBA ^d , EVN ^e
I17208 – 0014	174.8	VLBI ^c
Mrk231	172.1	EVN ^f , MERLIN ^h
Mrk273	153.9	EVN, MERLIN ^{h,i}
IC694(Arp229)	41.8	EVN ^g , MERLIN ^j

^a For all estimates we assume $q_0=0.5 \text{ km s}^{-1}$ and $H_0=h 75 \text{ km s}^{-1} \text{ Mpc}^{-1}$. ^b Lonsdale et al. (1998), ^c (Diamond et al., 1999), ^d (Trotter et al., 1997), ^e (Pihlström et al., 2001), ^f (Klöckner et al., 2002), ^g (Klöckner & Baan, 2001), ^h (Richards et al., 2000), ⁱ (Yates et al., 2000), ^j (Polatidis & Aalto, 2000)

galaxy shows a rather disturbed morphology with an optically thin tidal-tail extending from a fan-like plume up to 50 arcsec (1.3 mas = 1 pc) toward the south. The fan-like plume itself is 15 arcsec in size and possibly displays the rather complex structure of the inner part of the interaction region of two disk galaxies in a merging sequence. This central part of Mrk 273 shows prominent dust lanes and ionized gas and two distinct regions with strong optical emission lines indicating SBN/AGN activity. The optical emission lines show a low-luminosity LINER nucleus in the north of around 1 arcsec in size and a Seyfert 2 type nucleus 4 arcsec located toward the southwest (Colina et al., 1999). The Seyfert 2 nucleus has also been observed in the near-infrared (NIR), but it shows no radio detection from this possible dust-enshrouded AGN. Instead the radio observations of the nuclear region reveal an additional object with no NIR counterpart, that located toward the

southeast of the northern nucleus showing a jet-like morphology at high resolution possibly reflecting the outflow from a third nucleus (Knapen et al., 1997; Carilli & Taylor, 2000). The kinematic structure in the central region of Mrk 273 has been studied with line emission at various bands ([O III], HI, CO, & OH) revealing the kinematic structure of the northern and in the southeastern regions. These observations give evidence of a possible disk-like structure in the northern nucleus of less than 800 mas in size and faint HI absorption and CO emission toward the southeastern source (Colina et al., 1999; Schmelz et al., 1988; Downes & Solomon, 1998; Schmelz et al., 1987).

2. The Continuum Emission

The continuum emission of the central region of Mrk 273 has been mapped at 1.6 GHz by averaging the offline spectral channels and is shown in Figure 1. The displayed continuum image shows multiple sources in a region of 1 square arcsec matching the northern and the south eastern radio emission of the nuclear region.

The south eastern emission region splits into individual sources with one strong central component, a northern component, and two marginal detections toward the south. In analogy with existing VLBA observations of the southern region (1.3 GHz) at slightly lower resolution (50 mas), the EVN radio structure may partially resolve the more organized structure consisting of a bright central source with an amorphous jet toward the south west (Carilli & Taylor, 2000). The emission of the central component is characterized by a relatively flat radio spectrum between 1.6 and 5 GHz of $|\alpha| = 0.28$ suggesting synchrotron self-absorption. In combination with a high brightness temperature of 5×10^6 K and observed gas inflow (HI absorption) this source may qualify as the possible third nucleus in the central region of Mrk 273 participating in the merging event (Carilli & Taylor, 2000). The EVN observations have not detected any OH emission or absorption toward the southern source.

The northern radio emission in Mrk 273 (Fig. 1) shows two continuum peaks with brightness temperatures on the order of 10^6 K separated by 77 mas in east west direction. The western component shows brighter and slightly extended continuum emission. The steep spectral index in both sources between 1.3 and 1.6 GHz indicates a pure synchrotron spectra (Condon et al., 1991). The VLBA observations of that northern nucleus reveal that both sources are embedded in a diffuse emission structure extended over 500×300 mas resulting from a dominant starburst. The broad HI absorption (540 km s^{-1}) toward the western component in the northern nucleus of Mrk 273 supports the hypothesis of a weak radio AGN, whereas the eastern component shows a relatively narrow absorption line (Carilli & Taylor, 2000; Lonsdale et al., 1998).

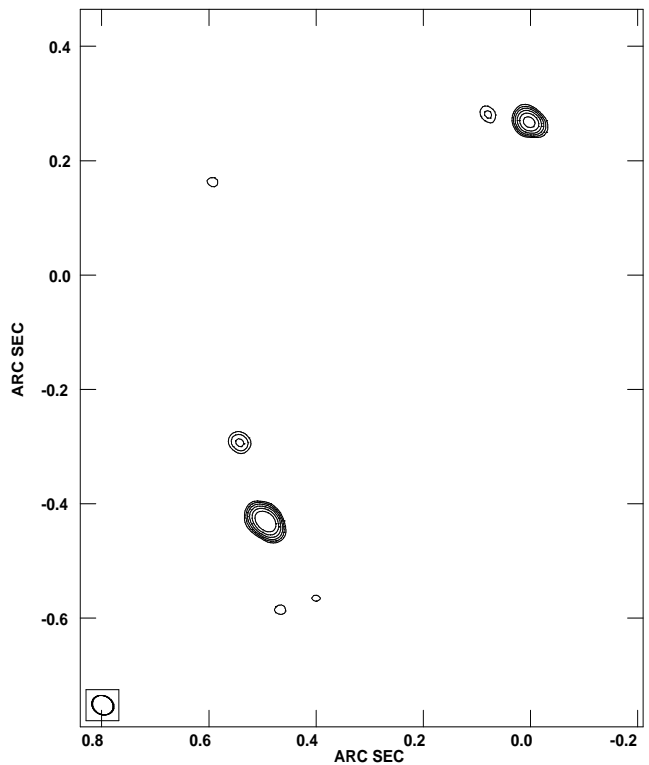


Fig. 1. Continuum emission of Mrk 273 observed with the EVN at 1.6 GHz at 40×30 mas resolution. The contour levels have a geometric progression in the square root of 2, hence every two contours implies a factor of two in surface brightness. First contour is $2.86 \text{ mJy beam}^{-1}$ corresponding to a 5.6σ level.

3. The Line Emission

Almost all OH emission is found near the eastern component of the northern nucleus and only marginal line emission has been detected toward the western part (see Fig. 2). Therefore the kinematic structure traced by the OH emission displays a different view of the velocity pattern in the northern nucleus than the HI observations. The integrated OH emission spectrum at the eastern source is shown in Figure 3 displaying a rather complex line structure covering a velocity range of almost 600 km s^{-1} . The spectrum displays slightly separated strong line features corresponding to the 1667 MHz hydroxyl emission and a weak line emission at 371 km s^{-1} offset to the brightest line feature reflecting the 1665 MHz line of the hydroxyl main-line emission. The emission itself is only partially superposed on the observed eastern continuum component and extends up to 75 mas toward the north (Fig 2). The spatial distribution of the OH suggests amplification of the continuum emission as a underlying background, supporting a classical amplification scheme (Baan, 1989). The estimated gain given by the ratio of the averaged line emission to the continuum emission is on the order of 14.

The overall line ratio of the detected hydroxyl main-line features of 17 is much higher than the LTE ratio of 1.8 and suggests optically thin maser emission with a more

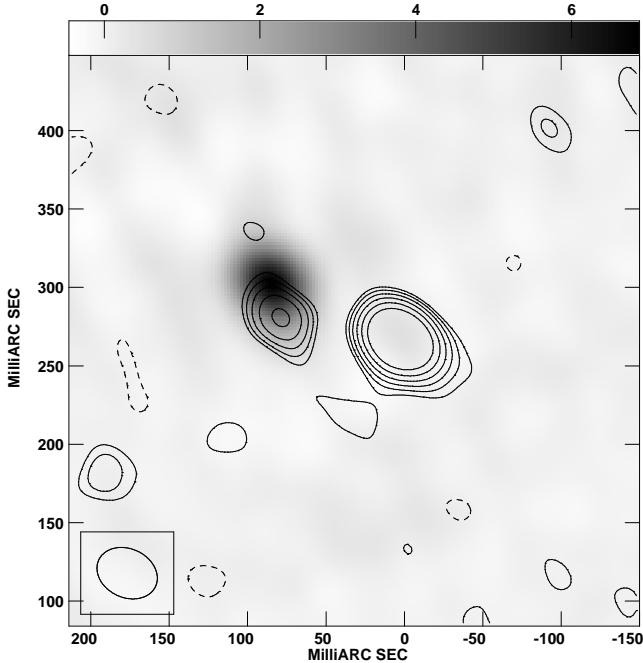


Fig. 2. A close-up of the northern nucleus in Mrk 273 showing the continuum emission in contours superposed on the integrated line emission in grey scale, observed with the EVN at 1.6 GHz at 40×30 mas resolution. The contour levels are a geometric progression in the square root of 2 starting at $0.14 \text{ mJy beam}^{-1}$.

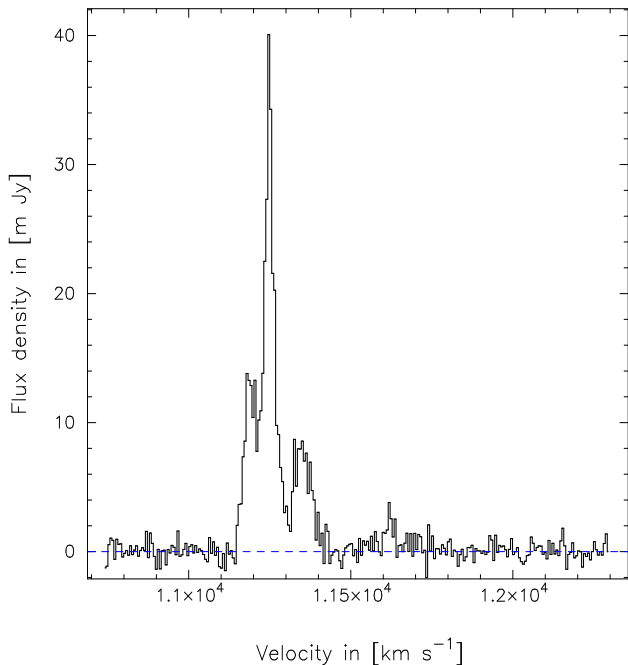


Fig. 3. Integrated line emission of Mrk 273 observed with the EVN. The strong line features are the 1667 MHz main-line emission and the weak emission line correspond to the 1665 MHz main-line. The velocity scale corresponds to a heliocentric velocity of the 1667 MHz line at 11328 km s^{-1} with a spectral resolution of 5.6 km s^{-1} .

complex pumping scheme, which implies a range of different physical conditions within the maser region. In order to reveal the physical conditions and the pumping scheme of the individual OH emission clouds, detailed modeling has to be done involving parameters such as OH abundances, kinetic gas temperature, dust temperature and physical extent. The OH column density has been estimated from the main-line ratio showing a high molecular content of $N_{\text{OH}} = 6.5 \times 10^{14} T_s [\text{cm}^{-2}]$ toward the eastern source of the northern nucleus. Compared with previous single-dish observations of the OH line, the EVN experiment detects around 70 percent of the 1667 peak flux density. The detected emission features clearly match the line structure of the low-resolution observations, which suggests that the dominant part of the maser emission is radiated within a central region of hundreds of parsecs. The 1665 MHz line emission has only been detected at a single region, which shows that almost all emission within the velocity range of 11450 to 11550 km s^{-1} has been missed by the EVN observations (Schmelz et al., 1987; Yates et al., 2000). The missing detection mirrors similar “non-detections” at high resolution, which suggests that the missing component relates to a more diffused and extended emission at scale sizes between kpc and parsec scales, corresponding to the resolution gap between the telescopes. The fact that the EVN observations shows almost an identical line pattern confirms that the missing emission component has a line width of several hundred km s^{-1} . A similar missing component has been observed toward the OH-MM galaxy Mrk 231 (Klöckner et al., 2002), which confirms that the extragalactic OH emission might have two emission components.

The velocity structure displayed by the OH emission shows a rather unexpected view of the kinematic structure as compared with the HI absorption measurements of the northern nucleus. The velocity structure traced by the HI absorption shows an east-west (increasing velocity) gradient over the entire region, whereas the OH emission reveals a north-south velocity gradient at the eastern edge of the overall velocity field (Cole et al., 1999). The line features in the integrated spectrum in Figure 3 splits into weaker emission lines with up to 90 km s^{-1} in width and suggest a molecular disk or TORUS in the eastern part of the nucleus. The kinematic structure is shown in the position-velocity diagram (Fig. 4) displaying two similar velocity patterns for both OH main-lines. The emission in the bottom of Figure 4 reflect the three major emission components from Figure 3 with the bright emission in the center and two weaker components at the edges. The decrease of the line intensity toward the outer edges of the kinematic structure is related to the maser amplification itself and has a geometry similar to the maser disks observed in H_2O Megamasers (e.g. NGC 4258: Greenhill et al., 1995). Furthermore, the velocity structure suggests an organized pattern of Keplerian rotation around a central object with no evidence of flattening at larger radii. The spatial extent and the overall north-south velocity

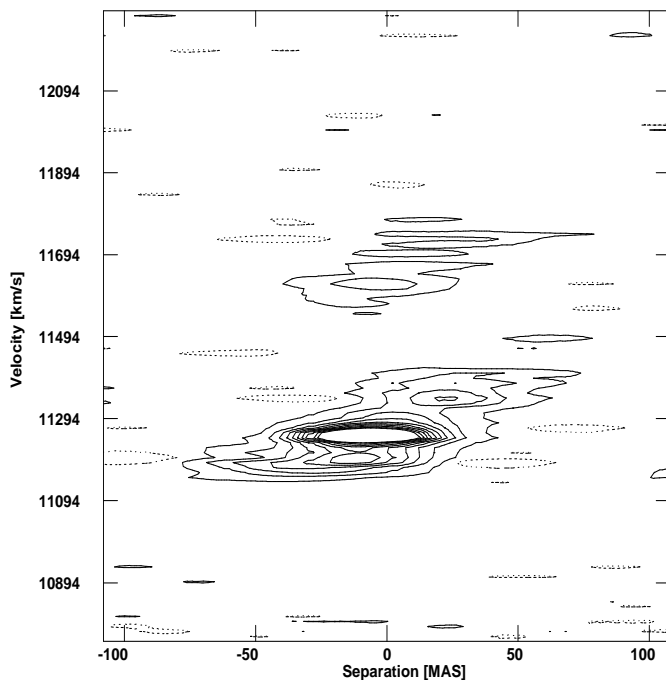


Fig. 4. The position–velocity diagram of Mrk 273 observed with the EVN, obtained along the major axis of the OH emission in north–south direction. The stronger emission correspond to the 1667 MHz OH line. The contours are in steps of 0.15 starting by 0.5 mJy beam⁻¹.

gradient of 1.5 km s⁻¹pc⁻¹ suggests an edge–on molecular disk/TORUS with a maximal size of 180 pc.

4. Conclusions

A significant result from these high–resolution observations of the molecular environment in Mrk 273 is that 70 percent of the single–dish emission has been detected in a region of around 180 pc in size revealing an edge–on disk or TORUS covering a weak radio nucleus. This nucleus has been thought to be a starburst nucleus, but these observations show that the binding mass of the central object is on the order of $3.5 \times 10^8 M_{\odot}$ suggesting a nuclear engine in the form of a BH. In this context the high–resolution observations of the broad HI absorption toward the second nucleus suggests that the northern nucleus of Mrk 273 possibly harbors two BHs at a projected distance of 66 pc. Furthermore, the missing maser emission supports the hypothesis, that the extragalactic hydroxyl emission results from two different phases of lower and higher density within the circumnuclear environment of Megamaser galaxies.

Acknowledgements. The European VLBI Network is a joint facility of European and Chinese radio astronomy institutes funded by their national research councils. This research was supported by the European Commission’s TMR Programme “Access to Large-scale Facilities”, under contract No. ERBFMGECT950012. We acknowledge the support of the

European Community - Access to Research Infrastructure action of the Improving Human Potential Programme and the EC ICN RadioNET (Contract No. HPRI-CT-1999-40003).

HRK thanks E. Loenen for special advice in Python programming.

References

- Baan W.A. 1989, ApJ 338, 804
 Baan W.A., Wood P.A.D., Haschick A.D. 1982, ApJ Lett. 260, L49
 Carilli C.L., Taylor G.B. 2000, ApJ Lett. 532, L95
 Cole G.H.J., Pedlar A., Holloway A.J., Mundell C.G. 1999, MNRAS 310, 1033
 Colina L., Arribas S., Borne K.D. 1999, ApJ Lett. 527, L13
 Condon J.J., Huang Z.P., Yin Q.F., Thuan T.X. 1991, ApJ 378, 65
 Diamond P.J., Lonsdale C.J., Lonsdale C.J., Smith H.E. 1999, ApJ 511, 178
 Downes D., Solomon P.M. 1998, ApJ 507, 615
 Greenhill L.J., Jiang D.R., Moran J.M., et al. 1995, ApJ 440, 619
 Klöckner H.R., Baan W.A. 2001, In IAU Symposium 206: Cosmic Masers: from protostars to blackholes; Eds. V. Migenes, E. Luedke
 Klöckner H.R., Baan W.A., Garrett G.A. 2002, A&A p. in prep.
 Knapen J.H., Laine S., Yates J.A., et al. 1997, ApJ Lett. 490, L29
 Lonsdale C.J., Lonsdale C.J., Diamond P.J., Smith H.E. 1998, ApJ Lett. 493, L13
 Pihlström Y.M., Conway J.E., Booth R.S., Diamond P.J., Polatidis A.G. 2001, A&A 377, 413
 Polatidis A.G., Aalto S. 2000, In 5th EVN Symposium 2000, Gothenburg, Sweden, Eds.: J.E. Conway, A.G. Polatidis, R.S. Booth, and Y.M. Pihlström, published Onsala Space Observatory, p. 127, pp. 127
 Richards A., Cohen, Cole, et al. 2000, In IAU Symposium 205: Galaxies and their constituents at the highest angular resolutions; Eds. R.T. Schilizzi, S.N. Vogel, F. Paresce, and M.S. Elvis
 Schmelz J.T., Baan W.A., Haschick A.D. 1987, ApJ 321, 225
 Schmelz J.T., Baan W.A., Haschick A.D. 1988, ApJ 329, 142
 Trotter A.S., Moran J.M., Greenhill L.J., Zheng X., Gwinn C.R. 1997, ApJ Lett. 485, L79
 Yates J.A., Richards A.M.S., Wright M.M., et al. 2000, MNRAS 317, 28